European Journal of Neuroscience, Vol. 23, pp. 3124–3138, 2006 doi:10.1111/j.1460-9568.2006.04774.x

Development of tinnitus-related neuronal hyperactivity through homeostatic plasticity after hearing loss: a computational model

Roland Schaette[1] and Richard Kempter[1,2,3]
[1]Institute for Theoretical Biology, Department of Biology, Humboldt-Universität zu Berlin, Invalidenstr. 43, 10115 Berlin, Germany
[2]Neuroscience Research Center, Charité, Medical Faculty of Berlin, Campus Charité Mitte, Berlin, Germany
[3]Bernstein Center for Computational Neuroscience Berlin, Berlin, Germany

Abstract

Tinnitus, the perception of a sound in the absence of acoustic stimulation, is often associated with hearing loss. Animal studies indicate that hearing loss through cochlear damage can lead to behavioral signs of tinnitus that are correlated with pathologically increased spontaneous firing rates, or hyperactivity, of neurons in the auditory pathway. Mechanisms that lead to the development of this hyperactivity, however, have remained unclear. We address this question by using a computational model of auditory nerve fibers and downstream auditory neurons. The key idea is that mean firing rates of these neurons are stabilized through a homeostatic plasticity mechanism. This homeostatic compensation can give rise to hyperactivity in the model neurons if the healthy ratio between mean and spontaneous firing rate of the auditory nerve is decreased, for example through a loss of outer hair cells or damage to hair cell stereocilia. Homeostasis can also amplify non-auditory inputs, which then contribute to hyperactivity. Our computational model predicts how appropriate additional acoustic stimulation can reverse the development of such hyperactivity, which could provide a new basis for treatment strategies.

Introduction

It is estimated that 2% of the general population suffer from chronic tinnitus (Pilgramm *et al*., 1999). The origin of this phantom percept, however, is not well understood, and therefore etiologic treatments are not available. Even though neural correlates of tinnitus have been found in animal studies, mechanisms for its development have not yet been identified.

In humans, tinnitus is often associated with sensorineural hearing loss (Henry *et al*., 1999). Behavioral studies indicate that animals also experience tinnitus after cochlear damage caused by acoustic trauma (Brozoski *et al*., 2002; Heffner & Harrington, 2002; Kaltenbach *et al*., 2004). Such damage to the auditory periphery leads to changes in neural activity in the auditory brainstem (Kaltenbach *et al*., 1998, 2000; Kaltenbach & Afman, 2000; Brozoski *et al*., 2002; Kaltenbach *et al*., 2004), the midbrain (Wang *et al*., 2002a), and the cortex (Seki & Eggermont, 2002, 2003; Noreña & Eggermont, 2003). Altered activity in the auditory cortex might therefore be a physiological correlate of tinnitus, but possibly not always its origin.

The earliest processing stage in the auditory pathway where tinnitus-related changes have been observed is the dorsal cochlear nucleus (DCN), which receives feedforward input from the auditory nerve (AN). Acoustic trauma leads to increased spontaneous firing rates in the DCN (Kaltenbach *et al*., 1998, 2000; Kaltenbach & Afman, 2000; Brozoski *et al*., 2002; Kaltenbach *et al*., 2004), and the degree to which the spontaneous rates are elevated is related to the strength of the behavioural evidence for tinnitus (Kaltenbach *et al*., 2004). Such hyperactivity occurs only in those regions of the DCN that are innervated by the lesioned parts of the cochlea (Kaltenbach *et al*., 2002). These experimental results present a paradoxical situation; cochlear damage leads to an overall decrease of AN activity, but the spontaneous firing rates in the DCN are increased.

Interestingly, hyperactivity in the DCN develops within days after hearing loss (Kaltenbach *et al*., 1998, 2000). Mechanisms of homeostatic plasticity also operate on this time scale (see, e.g. Turrigiano *et al*., 1998). Homeostatic plasticity is a response of neurons to sustained changes in their mean activity caused, for example, by changed mean synaptic drive. Homeostasis aims at stabilizing the mean firing rate of a neuron (Turrigiano, 1999; Burrone & Murthy, 2003) by scaling the strength of synapses and altering the intrinsic neuronal excitability (Turrigiano *et al*., 1998; Desai *et al*., 1999; Kilman *et al*., 2002). Such changes have been observed in the auditory cortex and in various regions of the auditory brainstem in response to sensory deprivation by means of cochlear ablation or cochlear damage through acoustic trauma: excitatory synaptic transmission was strengthened (Vale & Sanes, 2002; Muly *et al*., 2004; Kotak *et al*., 2005), inhibitory transmission was weakened (Suneja *et al*., 1998a, 1998b; Vale & Sanes, 2002; Kotak *et al*., 2005), and excitability was increased (Kotak *et al*., 2005).

To address the question of how peripheral hearing loss may lead to tinnitus-related hyperactivity of neurons in the auditory brainstem, we utilize a phenomenological model of the responses of AN fibers and downstream auditory neurons, for example in the cochlear nucleus (CN). The computational model is not intended to capture all known physiological details of the AN and the CN in detail. Instead we use a minimal model to demonstrate the basic mechanism of how homeostatic plasticity could contribute to the development of hyperactivity in response to altered input statistics. We therefore, for example, do not model single AN fibers but rather describe how the population firing rate of a group of AN fibers depends on the intensity of acoustic stimuli, and how the rate-intensity function of the population is altered by various kinds of cochlear damage.

Correspondence: Dr Richard Kempter, [1]Institute for Theoretical Biology, as above.
E-mail: r.kempter@biologie.hu-berlin.de

Received 8 December 2005, revised 17 February 2006, accepted 27 February 2006

Prolonged changes in the mean population activity of the AN are assumed to activate a compensation mechanism in a simple model of a downstream auditory neuron. A homeostatic readjustment of the mean rate of such a neuron, however, may also change its spontaneous firing rate. We derive the resulting 'steady state' spontaneous firing rate of the model neuron as a function of the amount of loss of inner hair cells (IHCs) and outer hair cells (OHCs) and the degree of damage to hair cell stereocilia (stereocilia damage, SD). Our results show that a homeostatic scaling reaction after cochlear damage can indeed lead to hyperactivity. We also consider model neurons that integrate auditory and non-auditory input. Homeostatic compensation of decreased excitatory drive from the AN can also boost the excitatory drive from additional non-auditory inputs, as homeostasis is a global mechanism that affects all synapses of a neuron. Therefore, non-auditory inputs can contribute to hyperactivity. For typical examples of cochlear damage as caused by acoustic trauma or cisplatin administration, we model spatial patterns of hyperactivity. The resulting hyperactivity patterns are similar to those observed experimentally in the DCN. Thus, our model for the development of hyperactivity through homeostatic plasticity suggests a possible mechanism for the development of tinnitus after hearing loss. Moreover, the theory predicts that hyperactivity could be alleviated by specially designed acoustic stimuli. These stimuli differ substantially from the unspecific broad-band noise stimuli commonly used in tinnitus therapy (Hazell, 1999) and could therefore constitute a basis for new treatment strategies.

Materials and methods

We have set up a phenomenological model of the acoustic environment as well as of the responses of the AN and downstream auditory neurons, for example in the CN. The model is phrased in terms of firing rates of small populations of AN fibers and CN neurons.

Distribution of sound intensities

We assume that the probability density function $p_I(I)$ of the sound intensity levels I (in units of dB) of a mixture of acoustic stimuli, like speech or other communication signals, environmental sounds, and background noise, is Gaussian, on average over hours to days:

$$p_I(I) = \frac{1}{\sqrt{2\pi\sigma_I^2}} \exp\left(-\frac{(I-\mu_I)^2}{2\sigma_I^2}\right). \quad (1)$$

We set the mean value μ_I of the intensity distribution to 40 dB. Standard deviations of 15 dB were reported for speech, 13 dB for vocalizations and 9 dB for environmental sounds (Escabi *et al.*, 2003). To capture the resulting, broader, intensity distribution of a mixture of these classes of sound events that may have different mean values, we choose the standard deviation σ_I of the intensity distribution to be 25 dB. Moreover, for simplicity we assume the same intensity distribution for all frequencies. This Gaussian distribution of sound intensity levels in dB corresponds to a long-tailed distribution of the linear amplitudes of the sound stimuli (see, e.g. Escabi *et al.*, 2003). The exact shape of the distribution, however, is not critical. All unimodal distributions where the majority of sound intensity levels is within the dynamic range of AN fibers yield similar results.

Auditory nerve responses

The population firing rate $f(I)$ of the AN at a sound intensity I is the average over a small population of AN fibers with different thresholds and spontaneous rates, but tuned to similar frequencies. In other words, we average over AN fibers with high spontaneous rates and low thresholds as well as AN fibers with low spontaneous rates and high thresholds. Such a population firing rate approximates the input of a downstream neuron that has synapses with a large number of AN fibers. We assume the same response function $f(I)$ for all frequencies. For simplification of the arguments, we choose $f(I)$ to be adapted to $p_I(I)$ so that $f(I)$ has maximum information on I if I is larger than some threshold I_{th}. For $I > I_{th}$, $f(I)$ is proportional to the normalized cumulative distribution function of $p_I(I)$: $\int_{I_{th}}^{I} p_I(I')\,dI'$ (infomax principle, Laughlin, 1981). For high I, $f(I)$ saturates at rate f_{max}. For $I < I_{th}$, there is spontaneous activity $f(I < I_{th}) = f_{sp}$, which occurs with probability: $P_{sp} = \int_{-\infty}^{I_{th}} p_I(I)\,dI$ (see also Fig. 2). To summarize, we have:

$$f(I) = \begin{cases} f_{sp} & \text{for } I < I_{th}, \\ \int_{I_{th}}^{I} p_I(I')dI' & \\ f_{sp} + (f_{max} - f_{sp})\dfrac{}{1 - P_{sp}} & \text{for } I \geq I_{th}. \end{cases} \quad (2)$$

Due to our infomax assumption, the distribution $p_f(f)$ of AN firing rates is flat for $f_{sp} < f \leq f_{max}$ and has a delta peak at frequency $f = f_{sp}$ (see Fig. 3b),

$$p_f(f) = P_{sp}\delta(f - f_{sp}) + \begin{cases} p_d & \text{for } f_{sp} < f \leq f_{max}, \\ 0 & \text{otherwise} \end{cases} \quad (3)$$

where $p_d = (1 - P_{sp})/(f_{max} - f_{sp})$ is the probability density of driven activity. The mean AN firing rate is: $\langle f \rangle = \int f' \cdot p_f(f')\,df'$. Using Eqn (3) we have:

$$\begin{aligned} \langle f \rangle &= P_{sp} f_{sp} + \int_{f_{sp}}^{f_{max}} f' \cdot p_d\,df' \\ &= P_{sp} f_{sp} + \frac{1}{2}(1 - P_{sp})(f_{max} + f_{sp}). \end{aligned} \quad (4)$$

Effects of cochlear damage on auditory nerve activity

The main parameters that influence AN responses in our model equations (Eqns 2 3, and 4) are the threshold I_{th}, which determines the probability of spontaneous activity, the spontaneous rate f_{sp}, and the maximum rate f_{max}. They are changed by cochlear damage.

We consider the effects of loss of inner and outer hair cells and of damage to the stereocilia of inner and outer hair cells. We denote the fraction of remaining IHCs by H_i, the fraction of remaining OHCs by H_o, and the fraction of undamaged stereocilia by S. The three parameters H_i, H_o and S vary between 1 (healthy) and 0 (loss of all hair cells or damage of all stereocilia). For simplification, we assume that our infomax assumption for the AN population response (see above) also holds in the case of cochlear damage.

The death of an IHC deprives the corresponding AN fibers of their input, because each AN fiber only contacts one IHC, and each IHC is contacted by 10–30 AN fibers (Ryugo, 1992). Moreover, the amplitude of the AN's compound action potential is reduced approximately proportional to the amount of IHC loss (Wang *et al.*, 1997; Salvi *et al.*, 2000). We therefore model the effect of IHC loss by a multiplicative reduction of the AN population firing rate. IHC loss then affects the spontaneous firing rate, $f_{sp}(H_i) = H_i f_{sp}$, and the

maximum firing rate of the AN, $f_{max}(H_i) = H_i f_{max}$ (see Fig. 2a). From Eqn (4) we find the mean AN firing rate after IHC loss,

$$\langle f(H_i)\rangle = H_i \cdot \langle f\rangle. \tag{5}$$

OHC loss is approximated by an increase in the AN threshold I_{th} in proportion to the amount of OHC loss, $I_{th}(H_o) = I_{th} + \Delta_o\,(1 - H_o)$ where $\Delta_o = 60$ dB is the threshold shift for the loss of all outer hair cells at $H_o = 0$ (Dallos & Harris, 1978; Harrison, 1981). Therefore, the probability of spontaneous firing is increased, $P_{sp}(H_o) \geq P_{sp}$ where $P_{sp}(H_o) = \int_{-\infty}^{I_{th}(H_o)} p_I(I)\,\mathrm{d}I$, and the probability density of driven activity is reduced to $p_d(H_o) = [1 - P_{sp}(H_o)]/(f_{max} - f_{sp})$. The spontaneous and the maximum discharge rates are not affected (Dallos & Harris, 1978; Schmiedt & Zwislocki, 1980). The resulting response curves for the population firing rate of the AN are steeper, as observed experimentally for single fibers (Harrison, 1981; see Fig. 2b). The mean firing rate is then given by:

$$\langle f(H_o)\rangle = P_{sp}(H_o) f_{sp} + \frac{1}{2}(1 - P_{sp}(H_o))(f_{max} + f_{sp}). \tag{6}$$

Noise-induced damage to the stereocilia of inner and outer hair cells increases the response threshold of AN fibers and decreases their spontaneous firing rate (Liberman & Dodds, 1984; Liberman, 1984). For a complete loss of all stereocilia ($S = 0$) the threshold is increased by $\Delta_S = 80$ dB, and the spontaneous rate is decreased by a factor of two-thirds (estimates based on Liberman & Dodds, 1984; Liberman, 1984). For intermediate degrees of stereocilia damage (SD) where $0 \leq S \leq 1$, we have $I_{th}(S) = I_{th} + \Delta_S \cdot (1{-}S)$, and $f_{sp}(S) = f_{sp}(1 + 2S)/3$. As for OHC loss, the probability of spontaneous activity depends on the amount of threshold shift, $P_{sp}(S) = \int_{-\infty}^{I_{th}(S)} P_I(I)\,\mathrm{d}I$, and the probability density of driven activity is then given by $p_d(S) = \frac{1 - P_{sp}(S)}{f_{max} - f_{sp}(S)}$.

Together with the decrease in spontaneous firing rate, we obtain:

$$\langle f(S)\rangle = P_{sp}(S) f_{sp}(S) + \frac{1}{2}(1 - P_{sp}(S))(f_{max} + f_{sp}(S)). \tag{7}$$

for the mean firing rate of the AN after SD.

If IHC and OHC loss, or SD and IHC loss, occur together, we assume that the different types of cochlear damage independently influence the parameters of the AN response function. For IHC and OHC loss, we then get the spontaneous rate $f_{sp}(H_i,H_o) = H_i f_{sp}$, the maximum rate $f_{max}(H_i,H_o) = H_i f_{max}$, and the threshold $I_{th}(H_i,H_o) = I_{th} + \Delta_o\,(1 - H_o)$. The mean firing rate of the AN population is:

$$\langle f(H_i, H_o)\rangle = H_i \cdot \langle f(H_o)\rangle, \tag{8}$$

where $\langle f(H_o)\rangle$ is given in Eqn (6). Similarly, for IHC loss and SD, we have the spontaneous firing rate $f_{sp}(H_i,S) = H_i f_{sp}(S)$, the maximum firing rate $f_{max}(H_i,S) = H_i f_{max}$, and the threshold $I_{th}(H_i,S) = I_{th} + \Delta_o\,(1 - S)$. The mean AN population rate is

$$\langle f(H_i, S)\rangle = H_i \cdot \langle f(S)\rangle, \tag{9}$$

where $\langle f(S)\rangle$ is given in Eqn (7).

Model for a downstream auditory neuron

Downstream auditory neurons, for example in the cochlear nucleus, are modelled as firing rate units with some nonlinear response function. Each model neuron receives excitatory input from the AN at a variable rate f, and a constant additional input from other sources at rate f_{add}. The sum of the two inputs is weighted by the adjustable synaptic gain factor g, and a response threshold θ is subtracted. The firing rate r of the model neuron is then:

$$r = R(f + f_{add}) = \begin{cases} r_{high} \cdot \tanh\left(\frac{g\cdot(f+f_{add})-\theta}{r_{high}}\right) & \text{for } g\cdot(f+f_{add}) \geq \theta, \\ 0 & \text{otherwise,} \end{cases} \tag{10}$$

where $r_{high} = 300$ Hz is the highest possible firing rate of the model neuron. The gain factor g is set to 1 for the initial, healthy condition. The threshold θ is set to $\theta = f_{add}$ to ensure that in the healthy case ($g = 1$) the model neurons have the same response distribution for different firing rates of the additional input (see Figs 3 and 5). The spontaneous firing rate of the model neuron is $r_{sp} = R(f_{sp} + f_{add})$, and the maximum firing rate is $r_{max} = R(f_{max} + f_{add})$.

The probability density function $q(r)$ of the model neuron's firing rates r is derived from the distribution $p_f(f)$ of AN responses and the response function R. The probability P_{sp} of spontaneous activity of the model neuron is the same as in the AN. In summary, we have:

$$\begin{aligned} q(r) &= \frac{1}{R'(R^{-1}(r))} p_f(R^{-1}(r)) \\ &= P_{sp}\cdot\delta(r - r_{sp}) + \begin{cases} \frac{p_d}{g}\cdot\frac{1}{1-(r/r_{high})^2} & \text{for } r_{sp} < r \leq r_{max} \\ 0 & \text{otherwise.} \end{cases} \end{aligned} \tag{11}$$

The mean firing rate of the model neuron is then given by:

$$\begin{aligned} \langle r\rangle &= \int_{r_{sp}}^{r_{max}} r'\cdot\, q(r')\,\mathrm{d}r' \\ &= P_{sp} r_{sp} + \frac{p_d}{g}\int_{r_{sp}}^{r_{max}} \frac{r'}{1 - (r'/r_{high})^2}\,\mathrm{d}r' \\ &= P_{sp} r_{sp} + \frac{r_{high}^2 p_d}{2g}\ln\frac{r_{high}^2 - r_{sp}^2}{r_{high}^2 - r_{max}^2}, \end{aligned} \tag{12}$$

where r_{sp} and r_{max} depend on g (see above) so that $\langle r\rangle$ increases with increasing g.

Homeostatic plasticity

Homeostatic plasticity serves to stabilize the mean activity of a neuron around a certain target level over long time scales on the order of days (Turrigiano, 1999; Burrone & Murthy, 2003). We model the effects homeostatic plasticity by a change in the gain factor g that is triggered by deviations of the mean activity $\langle r\rangle$ from a certain target rate r^*. We assume that the response function R is not affected by homeostatic plasticity, as in our model the adjustment of g is sufficient to mimic the changes in effective response gain by homeostatic scaling. The change of g that is necessary to restore the mean activity $\langle r\rangle$ in Eqn (12) to its target level r^* is computed numerically. The time-course of homeostatic plasticity is not considered. An upper limit of three (three times the normal gain) is imposed onto g to reasonably account for physiological constraints on synaptic strengths and excitability (see, e.g. Turrigiano *et al.*, 1998).

Additional acoustic stimulation

During the presentation of an acoustic stimulus at a suprathreshold intensity $I_{stim} > I_{th}$, the AN firing rate is $f_{stim} = f(I_{stim})$. If the stimulus is presented continuously, the spontaneous firing rate f_{sp} of the AN fiber population is to be replaced by $f_{stim} > f_{sp}$. The AN then fires at rate f_{stim} with probability $P_{stim} = \int_{-\infty}^{I_{stim}} p_I(I)\ dI$, that is whenever I_{stim} is higher than the intensity I of an environmental stimulus with distribution p_I. The mean firing rate $\langle r \rangle$ of a second-order model neuron can then be calculated using Eqn (12) with P_{sp} and f_{sp} replaced by P_{stim} and f_{stim}. If $\langle r \rangle$ differs from the desired value r^*, homeostatic plasticity is activated, and g is changed. After homeostasis, the value of g depends also on I_{stim}. The required stimulus intensity I^*_{stim} to reverse hyperactivity (see Fig. 8) is such that $g(I^*_{stim})$ after homeostasis leads to a normal spontaneous firing rate $r_{sp,healthy}$ in the second-order neuron when the additional stimulation is turned off, namely $R(f_{sp}, g(I^*_{stim})) = r_{sp,healthy}$. The calculation of I^*_{stim} is carried out numerically, and separately for each frequency channel.

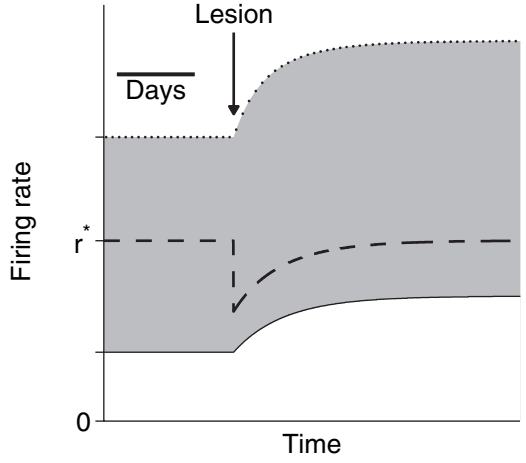

FIG. 1. Homeostatic stabilization of the mean firing rate of a neuron and hyperactivity. The grey area illustrates the range of firing rates from spontaneous (solid line) to maximum rate (dotted line) as a function of time. If for example a lesion suddenly decreases the mean firing rate (dashed line) without affecting the dynamic range of rates, a subsequent restoring of the mean rate to a target value r^* can lead to an increased spontaneous firing rate, or hyperactivity. Such a homeostatic stabilization could occur at many different levels in the auditory pathway as well as in other areas of the central nervous system.

Implementation

The model was implemented using MATLAB from the MathWorks Inc.

Results

The aim of this study was to demonstrate how a stabilization of neuronal activity through homeostatic plasticity could contribute to the development of hyperactivity in the auditory system after hearing loss. Figure 1 illustrates how homeostasis stabilizes a neuron's mean activity. We assume that, initially, some input drives the neuron to fire within a range between its spontaneous and maximum firing rates. The mean firing rate is determined by the statistics of the input signal. Let us focus on a case where after a lesion the statistics of the input changes such that the mean firing rate of the neuron is decreased without affecting the range of firing rates, a scenario that is reminiscent of the loss of outer hair cells in the cochlea. If homeostatic plasticity then restores the mean rate to its target value, for example by increasing synaptic efficacies, this can also increase the neuron's spontaneous firing rate, thus causing hyperactivity. Hyperactivity typically develops when the activity of the neuron is changed such that the ratio between the mean and spontaneous firing rate is reduced; further details of the activity statistics are not overly important. We now apply this concept to the first stages of the auditory pathway, using a phenomenological model of the responses of AN fibers and downstream auditory neurons in the CN.

Population firing rate of the auditory nerve

Based on various experimental studies, we describe auditory nerve activity by a population firing rate (black lines in Fig. 2), which is an average over several type-I AN fibers with similar characteristic frequencies. Being a population average, it comprises AN fibers with different spontaneous rates, thresholds, and dynamic ranges. We regard this as a reasonable approximation of the input of a downstream neuron that has synaptic contacts to many different AN fibers. The population response threshold is set to 0 dB SPL, which corresponds to the threshold of the most sensitive fibers. Below threshold there is

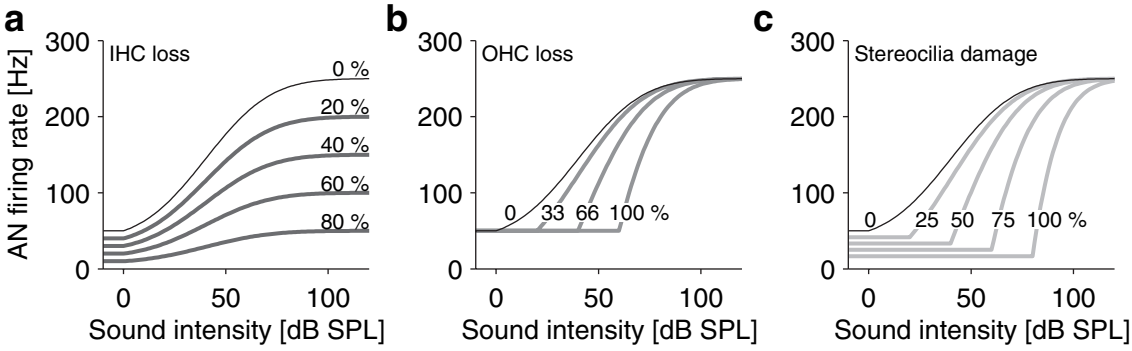

FIG. 2. Firing-rate model for a small population of AN fibers with similar characteristic frequencies. The population firing rate increases with increasing sound intensity. We model hearing loss caused by damage to or loss of cochlear hair cells. (a) Loss of IHCs scales down the AN population response (0% IHC loss, black line; 20, 40, 60, 80% loss, dark grey lines). (b) Loss of OHCs increases the response threshold (0% loss, black line; 33, 66, 100% loss, medium grey lines). (c) Damage to stereocilia of inner and outer hair cells increases the response threshold and decreases the spontaneous firing rate of AN fibers (0% damage, black line; 25, 50, 75, 100% damage, light grey lines).

spontaneous activity of 50 Hz, corresponding to an average over AN fibers with low and high spontaneous rates. For supra-threshold stimuli, the average population discharge rate grows with the stimulus intensity and saturates at 250 Hz. The dynamic range (20–80% rise) of the population response is 40 dB (Sachs & Abbas, 1974; Dallos & Harris, 1978; Liberman, 1978; Wang *et al*., 1997).

Damage to cochlear hair cells alters AN rate-intensity functions

Sensorineural hearing loss changes the response properties of the AN. We distinguish between hearing loss caused by loss of IHCs, loss of OHCs, and SD.

IHCs provide the main input to AN fibers. Each IHC is innervated by 10–30 AN fibers, but each AN fiber contacts only one IHC (Ryugo, 1992). Loss of IHCs therefore deprives associated AN fibers of their input, whereas the response properties of AN fibers associated with the remaining healthy IHCs seem largely unaffected (Wang *et al*., 1997). The degree of IHC loss is proportional to the decrease of the amplitude of the AN's compound action potential, i.e. the summed discharge of all AN fibers (Wang *et al*., 1997). We therefore model IHC loss by scaling down the rate-intensity function of the AN fiber population in proportion to the amount of IHC loss. This simplification of the effects of IHC loss implies that spontaneous as well as maximum rates of the population response are reduced, but the response threshold remains unchanged (Fig. 2a and Materials and methods before Eqn 5).

OHCs are thought to act as active amplifiers inside the cochlea (reviewed in Geisler, 1998). Pure loss of OHCs, for example induced by ototoxic agents, typically increases the threshold of AN fibers, while spontaneous and maximum discharge rate remain mostly unaffected (Dallos & Harris, 1978; Schmiedt & Zwislocki, 1980). We therefore model OHC loss by an increase in the response threshold of the fiber population, where the increase is proportional to the amount of OHC loss. Based on experimental studies, the loss of all OHCs is assumed to elevate the threshold by 60 dB. Moreover, OHC loss steepens the rate-intensity function of the AN fiber population and reduces its dynamic range (Fig. 2b and Materials and methods before Eqn 6).

Stereocilia couple inner and outer hair cells to the tectorial membrane. They are damaged by noise overexposure (see, e.g. Wang *et al*., 2002b), which can also cause a loss of hair cells. SD elevates the response threshold (Liberman, 1984; Heinz & Young, 2004) and decreases the spontaneous firing rate of AN fibers (Liberman & Dodds, 1984), but SD does not change the maximum discharge rate (Liberman & Kiang, 1984). We therefore model SD caused by noise overexposure by an increase of the response threshold and a decrease in the spontaneous firing rate of the rate-intensity function of the AN fiber population. Changes are assumed to be proportional to the degree of SD. From the experimental literature, we estimate that the threshold is elevated by 80 dB for severe loss of stereocilia (100% SD), and that the spontaneous rate is reduced by a factor of two-thirds (Fig. 2c and Materials and methods before Eqn 7). Similar to pure OHC loss, we assume a steepening of the rate-intensity functions also for SD, which might not always be the case (Heinz & Young, 2004; see Discussion). Our description of the effects of SD comprises damage to or loss of the stereocilia of IHCs and OHCs, and it also includes the effects of the loss of OHCs, because we assume that the total loss of an OHC's stereocilia has the same effect as the complete loss of an OHC.

In summary, each type of damage to the cochlea characteristically alters the rate-intensity function of the AN, which may trigger further changes along the auditory pathway.

Sensorineural hearing loss changes the distribution of AN firing rates

Before we can investigate the effects of homeostatic plasticity in downstream auditory neurons in response to sensorineural hearing loss, we first have to establish how the distribution of AN population firing rates is altered by cochlear damage. The fraction of time the AN population fires at some specific rate is determined by its rate-intensity function in conjunction with the distribution of sound intensities in an animal's environment. Let us assume that the sound intensity levels of acoustic stimuli obey a Gaussian distribution with 40 dB mean and 25 dB standard deviation, so that most of the intensities are within the dynamic range of AN responses (Fig. 3a, see also Materials and methods). We note that the Gaussian distribution of sound levels corresponds to a long-tailed distribution of the linear amplitudes of acoustic stimuli, as found for natural sounds (e.g. Escabi *et al*., 2003). Moreover, we assume that AN rate-intensity functions are tuned to the distribution of sound intensities so that the firing rates of the AN have maximum information on the sound intensity (infomax principle, Laughlin, 1981). This assumption is made in order to simplify further arguments and to allow an analytical approach (see Materials and methods). However, the detailed choice of the forms of both the rate-intensity function and the distribution of sound intensities are not critical for the main conclusions that can be drawn form our model; all unimodal distributions where the majority of sound intensity levels is within the dynamic range of the AN fibers yield similar results.

The probability density function of AN population rates for a healthy cochlea is shown in Fig. 3b (right panel). The probability of spontaneous AN activity is given by the fraction of time the sound intensity is below the response threshold of 0 dB. Therefore, the spontaneous firing rate of 50 Hz occurs with probability 0.05 (Fig. 3b, right panel, horizontal peak). For supra-threshold intensities, the probability density for firing at a given rate is constant in the interval between 50 and 250 Hz, due to our infomax tuning assumption. In the following, we are going to evaluate three examples of cochlear damage: 30% IHC loss, 66% OHC loss, and 50% SD. The amounts of damage were chosen for similar threshold elevation (OHC loss and SD), similar reduction of the mean AN rate (IHC and OHC loss), and similar reduction of the spontaneous AN firing rate (IHC loss and SD).

The effect of 30% IHC loss is illustrated in Fig. 3c. As IHC loss was assumed to scale down the whole AN population response, the range of firing rates is reduced and the mean firing rate is decreased in proportion to the amount of IHC loss. Furthermore, the spontaneous firing rate is lowered, but the probability of spontaneous activity is unchanged compared to the healthy case. The result of 66% OHC loss is shown in Fig. 3d. OHC loss elevates the response threshold of AN fibers, while the spontaneous and the maximum firing rate remain unchanged. As an elevated threshold renders more stimuli subthreshold, the probability of spontaneous activity is increased from 0.05 to 0.5, which simply means that epochs of spontaneous firing occur more often. Consequently, driven activity occurs less frequently, and this is why OHC loss decreases the mean firing rate of the AN. Finally, an example for 50% SD is given in Fig. 3e. The response threshold is elevated by SD, and therefore the probability of spontaneous activity is increased, similar to OHC loss. However, SD also decreases the spontaneous firing rate of the AN, while the maximum firing rate remains constant. Thus, epochs of spontaneous firing occur more often, but the firing rate within such an epoch is decreased. As a consequence, the mean AN population firing rate is decreased more strongly than for the same threshold shift caused by OHC loss.

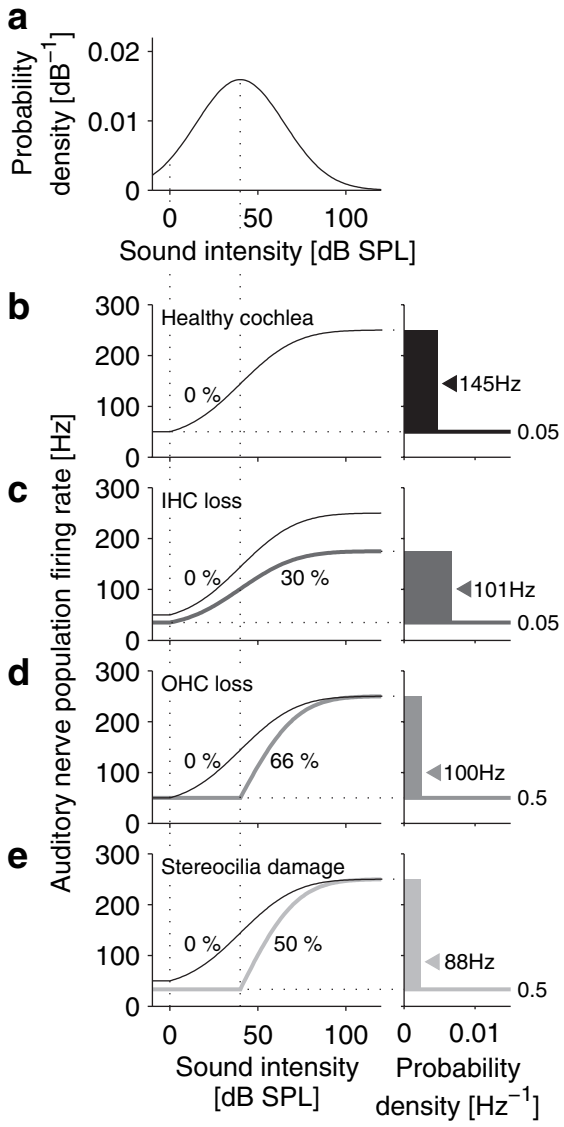

FIG. 3. Firing statistics of the AN model. (a) The distribution of sound intensity levels in units of dB is assumed to be Gaussian (40 dB mean, 25 dB standard deviation). (b–e, left panels) Rate-intensity functions of the AN population firing rate (b, healthy cochlea; c, 30% IHC loss; d, 66% OHC loss; and e, 50% SD). (Right panels) Firing-rate probability distributions of AN responses corresponding to the rate-intensity functions on the left and for the distribution of sound intensities in (a). Probability densities are on the abscissa, firing rates on the ordinate. The numbers at the horizontal 'delta' peaks of the distributions, e.g. 0.05 and 0.5, indicate the probability of occurrence of spontaneous activity for subthreshold stimuli. Shaded areas depict the distributions of firing-rate responses to super-threshold stimuli. Arrowheads denote mean firing rates. (b) Healthy cochlea (0% damage). Spontaneous activity is rare (probability 0.05). The range of firing rates is between 50 and 250 Hz. The mean activity is 145 Hz (arrowhead). (c) IHC loss (example 30%, dark grey) reduces spontaneous, mean (101 Hz) and maximum firing rates, while the probability of spontaneous activity remains at 0.05. (d) 66% OHC loss (medium grey) increases the AN response threshold by 40 dB without affecting the range of firing rates. Due to the threshold increase, the probability of spontaneous activity is increased to 0.5, and the mean firing rate is decreased to 100 Hz. (e) 50% stereocilia damage (light grey) increases the AN response threshold by 40 dB and decreases the AN's spontaneous (33 Hz) and mean firing rate (88 Hz). The probability of spontaneous activity is increased to 0.5.

To summarize, the loss of IHCs, loss of OHCs, and SD all decrease the mean population firing rate of the AN. This is achieved, however, in different ways. Most relevant for a development of hyperactivity in our model is that OHC loss and SD mainly increase the probability of spontaneous firing, whereas a loss of IHCs scales down the AN population response.

Homeostatic plasticity after hearing loss can lead to hyperactivity

Let us now evaluate how the responses of a model neuron are changed through hearing loss. The model neuron could represent a downstream auditory neuron in the CN that receives excitatory input from the AN. We assume that the model neuron is innervated by AN fibers with similar characteristic frequencies that are described by the mean population firing rate. The neuron is modelled as a firing rate unit with a nonlinear response function R that includes a gain factor g, which determines the impact of AN input on the model neuron's firing rates. The firing rate r of a model neuron in response to AN input at rate f is then given by $r = R(f) = r_{\mathrm{high}} \tanh (g \cdot f/r_{\mathrm{high}})$, with r_{high} being the maximum firing rate of the model neuron (see also Fig. 4a and b, and Materials and methods, Eqns 10–12).

We propose that a CN neuron has some target mean firing rate r^* (when averaged over days) that is stabilized by homeostatic plasticity. In the model, this rate stabilization is implemented through an adjustment of the gain factor g. This adjustment is in accordance with homeostasis through synaptic scaling (Turrigiano *et al*., 1998; Kilman *et al*., 2002) and neuronal excitability changes (Desai *et al*., 1999). Here, we do not model the dynamics of homeostatic plasticity, i.e. the time-course of g, but simply focus on the equilibrium state that is reached as a result of homeostasis. Let us now illustrate the consequences of a homeostatic stabilization of the model neuron's mean firing rate for the three examples of cochlear damage that we have introduced in Fig. 3.

IHC loss (30% in Fig. 4c) was argued to decrease mean, spontaneous and maximum firing rate of the AN, which, initially, also decreases the firing rate in the model neuron (Fig. 4c, panel $g = 1$). In order to counteract this decrease, homeostatic plasticity increases the model neuron's gain factor from $g = 1$ to some value $g > 1$. This restores the neuron's mean firing rate to its reference value r^*. Moreover, the neuron's reconstituted response distribution (Fig. 4c, panel $g = 1.43$) matches the one for 0% IHC loss (Fig. 4b, panel $g = 1$). Thus, moderate loss of IHCs can be fully compensated by homeostasis in the framework of our model.

OHC loss (66% in Fig. 4d), on the other hand, was argued to increase the probability of spontaneous activity in both the AN and the model neuron without changing the spontaneous firing rate. When homeostatic plasticity increases the gain factor g to counteract the decreased mean firing rate, the distribution of the model neuron's responses is drastically altered as compared to the healthy case. The maximum firing rate in the model neuron is elevated and, most importantly, also the spontaneous firing rate is increased (Fig. 4d, panel $g = 1.54$, see also Fig. 1).

SD (50% in Fig. 4e) was argued to increase the probability of spontaneous activity and to decrease the spontaneous rate in both the AN and the model neuron. Similar to OHC loss, homeostatic plasticity may recover the mean rate in the model neuron, but then the spontaneous rate is elevated as well (Fig. 4e, panel $g = 1.89$).

Thus, homeostatic compensation of OHC loss, for example after administration of ototoxic drugs, or SD as induced by noise overexposure can lead to increased spontaneous firing rates or hyperactivity of auditory neurons downstream of the AN.

Saturation of homeostasis decreases hyperactivity

In Figs 2 and 3 we have indicated that severe cochlear damage leads to low AN activity. If this is to be compensated by homeostasis in the

model neuron, large increases in response gain g would be needed. However, in a biological system, physiological constraints are likely to impose an upper limit on homeostatic scaling. We therefore explore the influence of an upper limit on the gain factor g, which is estimated to be $g_{max} = 3$ (based on results in Turrigiano *et al*., 1998). If this saturation limit is reached, homeostatic plasticity is not able to restore the mean firing rate of the model neuron.

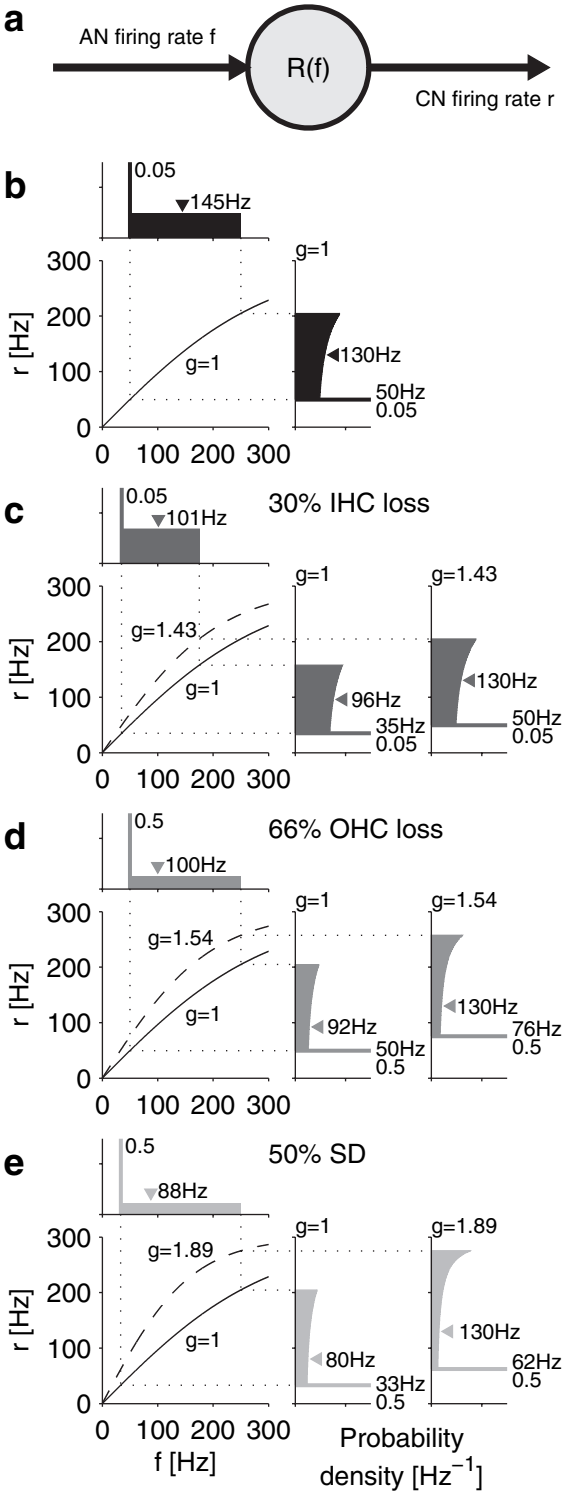

Figure 5 summarizes the effect of homeostasis and its saturation on the model neuron's activity for all degrees (0–100%) of hair cell loss or stereocilia damage. For IHC loss (Fig. 5a), homeostasis saturates at 67% loss. Below this limit, the spontaneous firing rate is restored to its normal value after homeostasis. Degrees of damage beyond the saturation limit lead to spontaneous firing rates of the model neuron that are even lower than normal. On the other hand, if AN activity is decreased by OHC loss (Fig. 5b), the saturation limit of homeostasis is never reached, at least not for the set of parameter values we found feasible to describe OHC loss. The neuron's spontaneous firing rate after homeostasis is thus a monotonically increasing function of the degree of OHC loss. Finally, SD can lead to saturation of homeostasis in the model neuron (Fig. 5c). Below the saturation limit of 67% SD, the neuron's spontaneous firing rate increases with increasing SD. If SD is larger than the saturation limit, the spontaneous firing rate decreases again. The maximum, or kink, of the neuron's spontaneous rate occurs at the saturation limit of homeostasis.

Non-AN input boosts the development of hyperactivity

Homeostatic plasticity is a mechanism that can scale all synapses of a neuron (Turrigiano, 1999). Therefore, a homeostatic increase in response gain to compensate for decreased AN activity could also influence non-auditory inputs. The CN receives input from a variety of other brain regions in addition to feedforward input from the AN. The most diverse set of such additional inputs is found in the DCN. There are projections from the contralateral CN (Cant & Gaston, 1982; Shore *et al*., 1992), top-down connections from the cortex (Weedman & Ryugo, 1996; Jacomme *et al*., 2003), and inputs from the somatosensory system (Kanold & Young, 2001; Zhou & Shore, 2004).

To evaluate the consequences of non-auditory input to the model neuron, we simply consider a constant excitatory input f_{add} in addition to the variable input f from the AN (Fig. 6a). Both inputs are scaled by the gain factor g so that the model neuron's rate reads $r = R(f + f_{add}) = r_{high}\tanh([g\cdot(f + f_{add} - \theta]/r_{high})$, where we have introduced a response threshold θ. We set this threshold to $\theta = f_{add}$

FIG. 4. Model for a downstream auditory neuron in the cochlear nucleus (CN) and illustration of the result of homeostatic plasticity. (a) The model neuron receives excitatory input at rate f from a population of AN fibers. The model neuron's output firing rate $r = R(f) = r_{high}\tanh(g \cdot f/r_{high})$ is determined by the response function R with its adjustable gain factor g and constant maximum firing rate $r_{high} = 300$ Hz. Homeostatic plasticity adjusts the mean of the output rate r by changing the gain factor g. (b) Healthy cochlea (no damage). The probability of AN fibers to fire at a given rate (top; identical to Fig. 3B) is mapped by the response function (bottom left) to the firing probability of the model neuron (right panel). The neuron's mean firing rate is 130 Hz (arrowhead), the spontaneous firing rate is 50 Hz, and the maximum firing rate is 205 Hz (horizontal dotted lines). The probability 0.05 of spontaneous firing in the model neuron is the same as in the AN. All probability distributions are at identical scales. (c–e) Same as in (b), but for different types of damage to the cochlea (grey), both before ($g = 1$) and after homeostasis ($g > 1$). (c) 30% IHC loss (dark grey) decreases the mean firing rate of the model neuron to 96 Hz and the spontaneous firing rate to 35 Hz (panel $g = 1$). Homeostatic plasticity increases the gain to $g = 1.43$ (dashed line in bottom left panel), which fully restores the neuron's response distribution (see b). (d) 66% OHC loss (medium grey) increases the probability of spontaneous activity to 0.5 without affecting the range of firing rates. The mean firing rate of the model neuron is decreased to 92 Hz (panel $g = 1$). Homeostasis increases the gain to $g = 1.54$ (dashed line in bottom left panel), but this substantially alters the neuron's response distribution (panel $g = 1.54$). Especially, the spontaneous firing rate is increased from 50 to 76 Hz. (e) 50% SD (light grey) decreases the mean firing rate in the model neuron to 80 Hz and the spontaneous firing rate to 33 Hz (panel $g = 1$). After homeostasis (panel $g = 1.89$), the spontaneous firing rate is increased to 62 Hz.

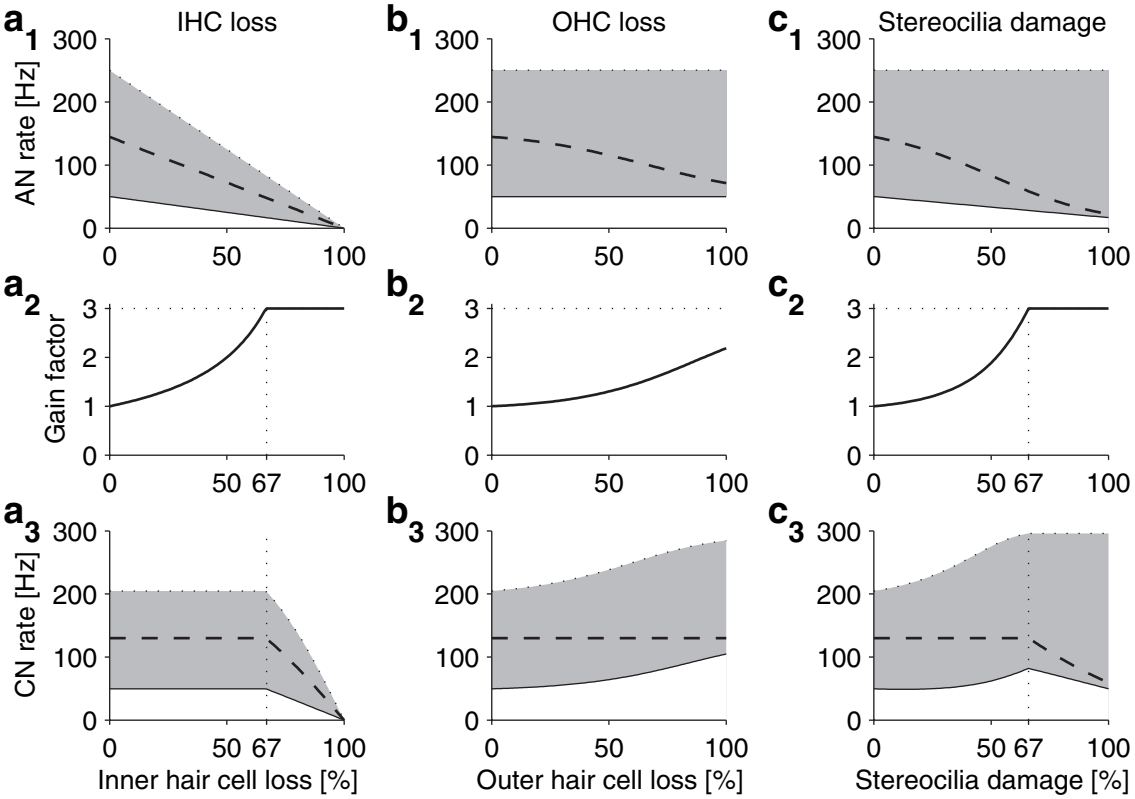

FIG. 5. AN activity, gain factor, and CN activity after homeostasis in dependence upon the degree of IHC loss, OHC loss, and SD. (a_1–a_3) IHC loss. (a_1) AN firing rates. Spontaneous (solid line), mean (dashed line), and maximum (dotted line) firing rate are reduced in proportion to the amount of IHC loss. The shaded area illustrates the range of firing rates. (a_2) Gain factor after homeostasis. Homeostatic scaling saturates because we have imposed an upper bound on the gain factor (here: $g_{max} = 3$). (a_3) CN model neuron firing rates after homeostasis. The mean firing rate (dashed line) is restored to its healthy value for up to 67% IHC loss. Beyond this limit, when homeostasis is saturated, the neuron's rates decrease with increasing loss of IHCs. (b_1–b_3) OHC loss. (b_1) The mean activity of the AN decreases with increasing OHC loss, but the range of firing rates, from spontaneous to maximum rate, remains constant. (b_2) The gain factor after homeostasis increases with increasing OHC loss. (b_3) The model neuron's mean rate is restored to its target value for all degrees of OHC loss, but the spontaneous firing rate is increased. (c_1–c_3) Stereocilia damage (SD). (c_1) Mean and spontaneous AN firing rates are decreased by SD. (c_2) The gain factor saturates for more than 67% SD. (c_3) The mean firing rate in the model neuron is restored to its target value for up to 67% SD, and the spontaneous activity is increased. For larger amounts of SD, the mean and spontaneous rate decline; the maximum rate stays constant.

so that the previous scenario without additional input in Figs 3–5 can be directly compared to the scenario with additional input in Fig. 6. For the healthy case with $g = 1$, both scenarios are identical (Fig. 6b). For homeostatic scaling that leads to $g > 1$ however, additional excitatory input to the model neuron gives rise to marked differences that depend on the type of cochlear damage.

We found that IHC loss can also lead to hyperactivity if there is additional excitatory input to the model neuron (Fig. 6c). The higher the firing rate of the additional input the more hyperactivity. Moreover, the saturation point of homeostasis is shifted towards greater damage. The situation is different for OHC loss; the results obtained with additional input are very similar to those obtained without (Fig. 6d). For SD, the model with additional input exhibits higher spontaneous firing rates after homeostasis than the model without. Also, the saturation point of homeostasis is shifted towards greater damage (Fig. 6e).

In conclusion, when the activity of the AN, which provides excitatory input to the CN, is reduced because of cochlear damage, homeostatic plasticity increases the effective response gain that affects all inputs. Therefore, additional non-auditory inputs are also amplified and then contribute to hyperactivity. This mechanism suggests how, for example, somatosensory input could be involved in the generation of tinnitus.

Model results for cochlear pathologies associated with tinnitus

In humans, acoustic trauma and treatment with cisplatin (used in cancer therapy) are often associated with tinnitus. Animal studies demonstrate that both acoustic trauma and cisplatin administration damage cochlear hair cells and lead to hyperactivity of DCN neurons (Kaltenbach *et al*., 1998, 2000; Brozoski *et al*., 2002; Kaltenbach *et al*., 2002, 2004). We are now going to present results of our model for the corresponding characteristic patterns of cochlear damage, where combinations of OHC and IHC loss, or SD and IHC loss, concurrently influence the AN population response (see Materials and methods, Eqns 8 and 9). We therefore consider a tonotopic array of CN neurons receiving input from the corresponding tonotopic loci of the cochlea via the AN (Fig. 7a).

Systemic cisplatin administration can cause severe OHC loss in the basal segment of the cochlea that responds to high frequencies, whereas IHCs are typically only affected to a limited degree (Kaltenbach *et al*., 2002; van Ruijven *et al*., 2004). Additionally, cisplatin can lead to a demyelination of AN fibers innervating the basal turn of the cochlea (van Ruijven *et al*., 2004, 2005). Therefore, in our framework we approximate the effects of cisplatin-induced combined damage to IHCs and AN fibers by moderate IHC loss. As for the spatial pattern of cochlear damage, we consider severe OHC

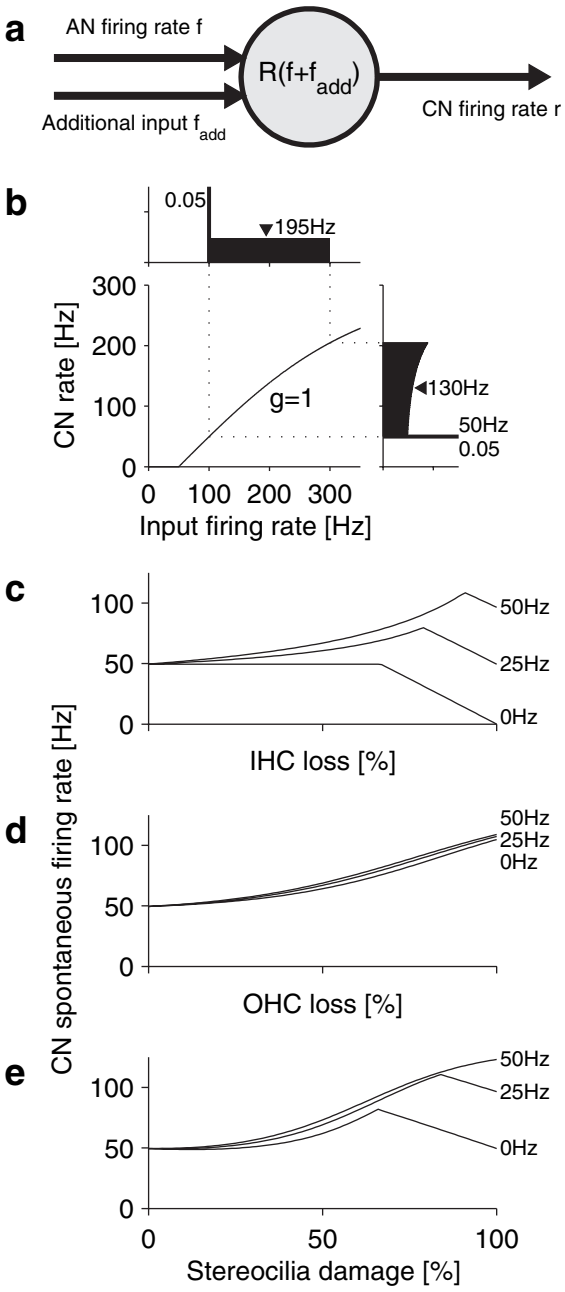

FIG. 6. Effects of additional input on hyperactivity. (a) The model neuron receives excitatory input from a population of AN fibers at variable rate f and from additional, non-auditory input fibers at constant rate f_{add}. The model neuron's output firing rate is $r = R(f + f_{add}) = r_{high} \tanh([g \cdot (f + f_{add} - \theta]/r_{high})$, with $\theta = f_{add}$ being the response threshold. (b) Healthy cochlea, $g = 1$. (Top) Distribution of the input $f + f_{add}$, with $f_{add} = 50$ Hz. (Bottom left) Response function R and (bottom right) response distribution of the DCN neuron for $g = 1$ (identical to the one without additional input in Fig. 4B). (c) Spontaneous firing rate of the model neuron after IHC loss and homeostasis for different values of f_{add} (0, 25, and 50 Hz). With additional input, hyperactivity also occurs after IHC loss, and the saturation point of homeostasis (kink in the curve) is shifted towards greater IHC loss. (d) For OHC loss, hyperactivity only weakly depends on f_{add}. (e) For SD, the maximum increase in spontaneous firing rate depends on the value of f_{add}, and the saturation point of homeostasis is shifted towards greater damage.

loss and moderate IHC loss in the basal parts of the cochlea (Fig. 7b). In the model, homeostasis then leads to hyperactivity in those neurons that receive input from the damaged parts of the cochlea (Fig. 7c). Moderate IHC loss (i.e. cisplatin-induced damage to IHCs) in addition to severe OHC loss lowers the spontaneous firing rates, but only in the model without additional input. Similar observations have been made in the DCN of animals after cisplatin administration, where strong increases in spontaneous activity were observed for pure OHC loss, and smaller increases when additional IHC damage occurred (Kaltenbach *et al*., 2002).

Noise overexposure or other forms of acoustic trauma induce severe damage to the stereocilia of inner and outer hair cells that extends over large parts of the cochlea up to the basal end. Acoustic trauma also causes OHC and IHC loss. The spatial extent of OHC loss is generally similar to that of SD, whereas IHC loss is typically less severe and restricted to smaller parts of the cochlea (Meleca *et al*., 1997; Chen & Fechter, 2003). In our model, we therefore evaluate a pattern of cochlear damage with severe SD (note that our description of SD also includes the effects of OHC loss), and moderate IHC loss (see Fig. 7d). The observed pattern of hyperactivity after homeostatic plasticity heavily depends on the amount of non-auditory additional input to the model neurons. Without additional input, the spontaneous firing rate is only elevated at a single peak that is associated with the edge of the stereocilia lesion (Fig. 7e, upper panel, $f_{add} = 0$ Hz). The peak structure is caused by the saturation of homeostasis (compare Fig. 5c). At frequencies where IHCs are lost in addition to severe SD, spontaneous firing rates can be even lower than before. With increasing additional input (25 and 50 Hz in Fig. 7e, upper panel), the peak in the spontaneous firing rate profile is shifted towards higher frequencies because homeostasis saturates at greater damage. Moreover, the peak becomes broader for 25 Hz additional input to finally extend over large parts of the tonotopic array for 50 Hz, at which the spontaneous firing rate is strongly elevated for all neurons that receive input from the damaged regions of the cochlea. The latter hyperactivity profile for 50 Hz additional input is similar to those observed experimentally in the DCN after severe unilateral acoustic trauma (Kaltenbach *et al*., 1998, 2000, 2004).

Hyperactivity caused by unilateral acoustic trauma was shown to persist even after cochlear ablation (Zacharek *et al*., 2002). Spontaneous firing rates were decreased by the ablation, but remained increased compared to the healthy case. To capture this experiment in the model, we first let homeostasis increase the model neuron's gain to compensate for the effects of acoustic trauma. Then we remove all AN activity, leaving only the additional input (50 Hz in our example). As homeostasis is a slow process, the gain remains adjusted to acoustic trauma for at least several hours after the ablation. The additional input is thus amplified, leading to spontaneous firing rates in the model that are reduced compared to the situation before the ablation (Fig. 7e, lower panel, 'ablated'), but still elevated, and the distribution of spontaneous rates reflects the pattern of cochlear damage. After longer waiting times on the order of days, homeostatic plasticity adapts the neuron's gain to the only remaining input f_{add}. In the model, f_{add} is constant across frequencies, leading to a flat profile of elevated spontaneous firing rates (dotted line in Fig. 7e, lower panel) when homeostasis is saturated at its upper bound. In experiments, the equilibrium distribution of spontaneous firing rates after AN section will depend on the distribution and activity of additional inputs across frequency channels in the auditory system.

Reversing hyperactivity through additional acoustic stimulation

Having established how hyperactivity and possibly tinnitus could develop through homeostatic plasticity after hearing loss, we are now able to evaluate how the pathologic changes could be reversed through additional sensory stimulation. It is obvious that hyperactivity could

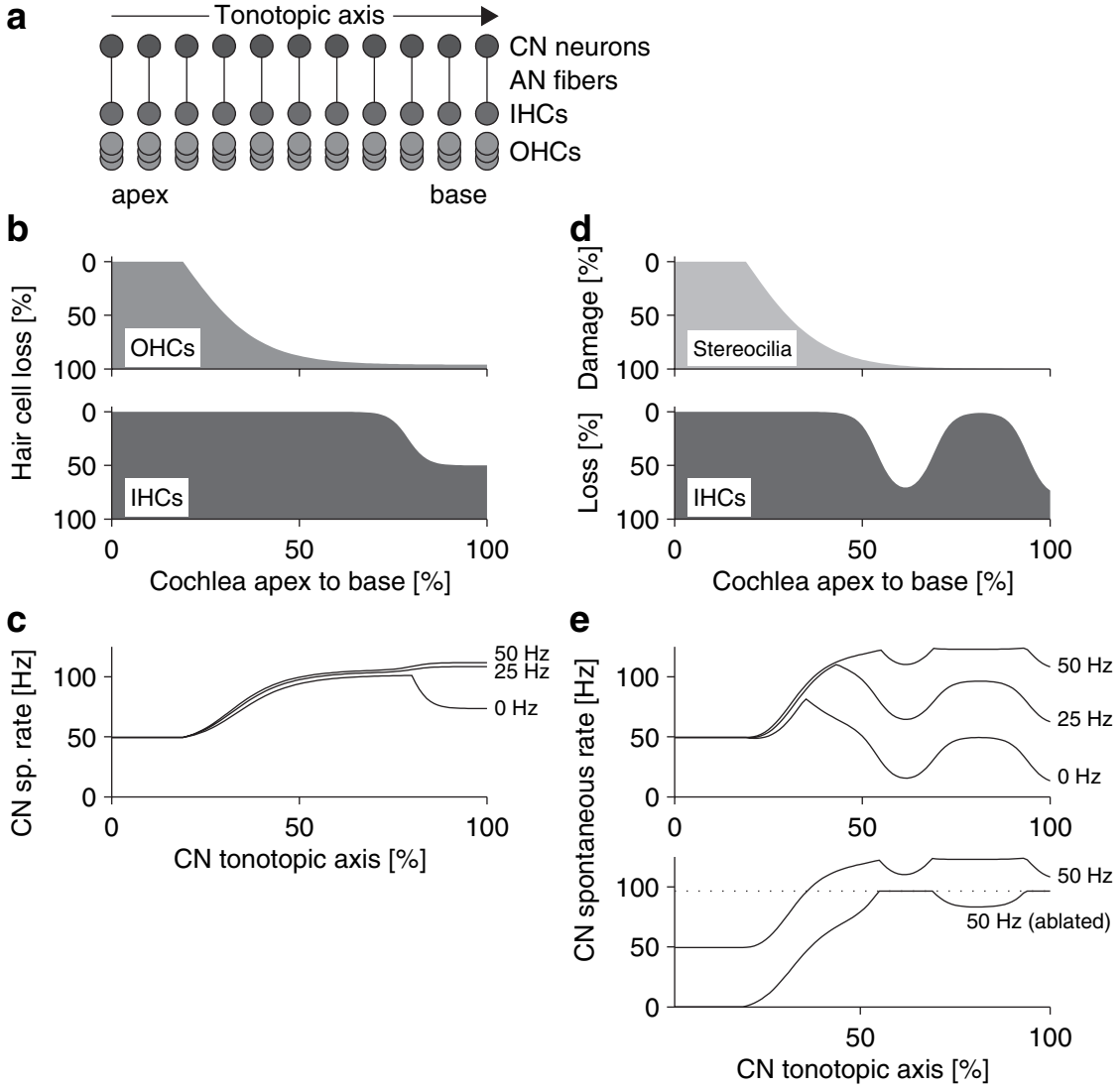

FIG. 7. Two examples of model results for cochlear pathologies that can lead to tinnitus in humans. (a) Illustration of the tonotopic connection between cochlea and CN. (b) Cochleograms indicate damage induced by systemic cisplatin administration. OHC loss extends over large parts of the cochlea (top panel). Additional damage to IHCs and AN fibers is approximated in our model by moderate IHC loss (bottom panel). (c) Spontaneous activity of CN model neurons after homeostasis as a function of a neuron's location along the tonotopic axis for three different rates (0, 25, and 50 Hz) of the additional input. Hyperactivity is observed in those model neurons that receive input from regions of the cochlea where OHCs are lost. Without additional input, extra IHC loss leads to lower spontaneous firing rates than the same amount of OHC loss alone. (d) Cochlear damage through noise-induced hearing loss. Stereocilia are severely damaged over large parts of the cochlea (top panel). IHC loss is less pronounced (bottom panel). (e) CN spontaneous rate after homeostasis. (Top panel) The amount and extent of hyperactivity heavily depends on the strength of the additional input, ranging from a single peak associated with the edge of the cochlear lesion for $f_{add} = 0$ Hz to strongly elevated spontaneous firing rates over large parts of the tonotopic axis for $f_{add} = 50$ Hz. Peak-like structures are caused by the saturation of homeostasis. (Bottom panel) For strong additional input (here 50 Hz), hyperactivity can persist after cochlear ablation. Immediately after the ablation, the profile still reflects cochlear damage (lower solid line), but later turns into a flat profile for the chronic case (dotted line).

be reversed in our model by restoring the regular distribution of AN firing rates, which corresponds to a perfect 'hearing aid'. A simpler and feasible way, however, would be permanent additional stimulation through specially adjusted noise devices. Let us now discuss the effects of different stimulation strategies on hyperactivity in our model. We evaluate a white-noise stimulus, as often used in tinnitus therapy (Hazell, 1999), and a specially designed matched-noise stimulus for an example of noise-induced hearing loss with severe stereocilia damage that strongly elevates hearing thresholds in the high-frequency range (Fig. 8a, upper panel). We employ the model variant without additional input, as it exhibits a distinct peak in the spontaneous firing-rate profile after homeostatic plasticity, which could be interpreted as the basis for a tone-like tinnitus sensation (Fig. 8a, lower panel). The peak is caused by the saturation of homeostasis (see also Figs 6e and 7e).

We first explore white-noise stimulation at 40 dB (Fig. 8b). Above ~3 kHz it is below the hearing threshold. The mean AN firing rate is increased by the additional stimulation only in the low-frequency range (not shown), where homeostatic plasticity then decreases the gain in the model neurons to compensate for the increased AN input (Fig. 8b, middle panel). Neurons in the high-frequency range are not affected, and the hyperactivity peak is unchanged. During stimulation, the white-noise stimulus evokes firing rates in the model neurons that are higher than those at the hyperactivity peak, possibly masking the

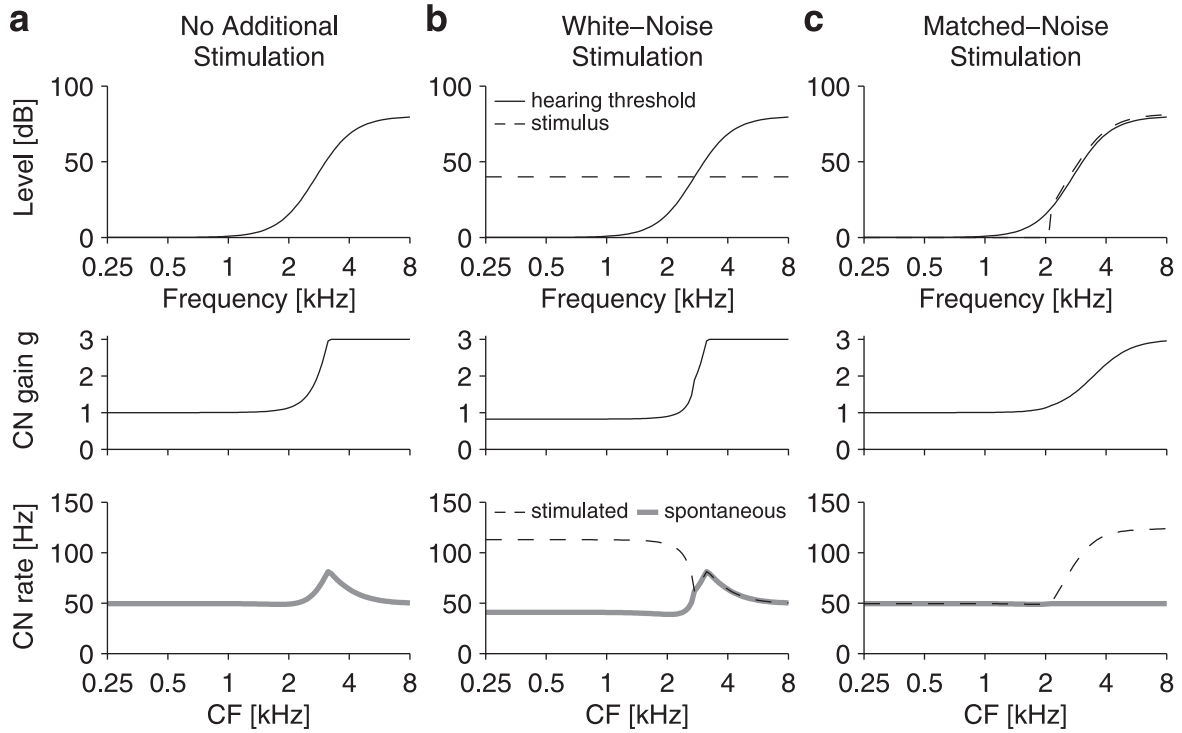

FIG. 8. Effects of sound stimulation on hyperactivity of CN model neurons. Each of the three top panels shows the hearing threshold curve for a case of severe noise-induced high-frequency hearing loss (solid lines) modelled through SD. We also depict levels of different acoustic stimuli (dashed lines). Let us consider the case when homeostatic plasticity has adapted the CN neurons to AN input evoked by a mixture of an additional sound stimulus (if applied) and ambient sounds. The resulting gain factors of CN model neurons in dependence upon the neurons' characteristic frequency (CF) are shown in the middle panels. The bottom panels show the corresponding spontaneous (thick grey lines) and stimulation-evoked (dashed lines) firing rates of the model neurons. (a) No additional stimulation. After homeostasis, there is a peak in the spontaneous firing rate profile of the CN where the gain g is saturated, reminiscent of a tone-like tinnitus. (b) 40 dB white-noise stimulation as often used for tinnitus masking. The stimulus is below the hearing threshold above ~3 kHz. During stimulation, evoked firing rates in the low-CF neurons are higher than those at the 'tinnitus frequency', possibly masking the percept. Immediately after switching off the white-noise stimulation, the hyperactivity peak in the firing rate profile is even more pronounced than without stimulation (see a). (c) Matched-noise stimulation. The stimulus is slightly above (1.5–4 dB) the hearing threshold in the severely impaired high-frequency range. After homeostasis, the stimulus evokes moderate firing rates in the high-CF neurons. Immediately after switching off the matched-noise stimulation, the profile of spontaneous firing rates across the tonotopic axis is flat, the hyperactivity peak is gone.

tone-like tinnitus (Fig. 8b, lower panel, dashed line). Immediately after the white-noise stimulus is turned off, however, the hyperactivity peak is even more pronounced (Fig. 8b, lower panel, thick grey line) than before the additional stimulation (see Fig. 8b), as the homeostatic adaptation has lowered the gain in the low-frequency range and thus has decreased the spontaneous firing rates there. An unspecific white-noise stimulus therefore masks a hyperactivity peak in the model, but even exaggerates it after the stimulus is turned off.

In a second scenario, we derive a matched-noise stimulus (see Materials and methods) that reverses hyperactivity and leads to a flat profile of the spontaneous firing rate across the tonotopic axis of the model neurons after homeostasis, as in the healthy situation (Fig. 8c, upper panel). This stimulus is 1.5–4 dB above the hearing threshold only in the high-frequency range, where hearing is impaired, and therefore increases the mean firing rate of AN fibers in this frequency range. As a consequence, homeostatic plasticity is triggered in those model neurons receiving input from the additionally stimulated AN fibers, where it lowers the pathologically increased gain factors. After homeostasis, the matched-noise stimulus evokes low to medium firing rates in the model (Fig. 8c, lower panel, dashed line), thus homeostasis does not suppress the response to the stimulus. Once stimulation is turned off, the spontaneous firing rate profile across the tonotopic axis is flat (Fig. 8c, lower panel, thick grey line). Hyperactivity would only slowly reemerge after prolonged periods without stimulation, and the time-course of reemergence is governed by the time-scale of days of homeostatic plasticity. It may therefore be possible to find a stimulation paradigm where intervals with and without stimulation are interleaved, which provides an efficient suppression of hyperactivity without the necessity of constant stimulation.

The observation that in our model additional acoustic stimulation can reverse hyperactivity is matched by the findings that hearing aids (Surr *et al*., 1999), noise devices (Schneider *et al*., 1999), and cochlear implants (Ito & Sakakihara, 1994; Quaranta *et al*., 2004) can reduce perceived tinnitus severity. Our matched-noise stimulus, however, is different from common masking approaches with unspecific broadband stimuli as it is designed not solely to mask tinnitus, but to decrease elevated spontaneous activity that constitutes the basis for the tinnitus sensation.

Discussion

We have presented a phenomenological model of the early auditory pathway to assess the question of how sensorineural hearing loss could lead to pathologically increased spontaneous firing rates (hyperactivity) in the auditory brainstem, which may be perceived as tinnitus. There are, to our knowledge, no other models on the development of tinnitus-related hyperactivity through homeostatic plasticity. Our model is based on a simplified description of the firing-rate response of AN fibers to acoustic stimuli, the effects of hearing loss through damage to cochlear hair cells, the responses of downstream auditory

neurons in the CN to input from the AN and other sources, and the effect of a homeostatic plasticity mechanism that stabilizes the mean firing rate of CN neurons at a constant level.

In the healthy auditory system, homeostatic plasticity could help to ensure that auditory neurons are active within the right range of firing rates independent of the prevailing acoustic environment. Homeostatic plasticity in auditory neurons might also prevent us from perceiving spontaneous neuronal activity as sound. For pathologically altered processing in the cochlea, however, this plasticity mechanism could also have detrimental effects. We propose that homeostatic plasticity can lead to hyperactivity in cochlear nucleus neurons when the ratio between the spontaneous and the mean firing rate in the AN is decreased. As sensorineural hearing loss always lowers the mean firing rate in the AN, the relative change of the spontaneous rate is crucial. We found that in a generic model of IHC loss that preserves the ratio of mean and spontaneous activity in the AN, restoring of the activity statistics of second-order neurons is possible. Because both OHC loss and SD decrease the ratio between the mean and the spontaneous firing rate of the AN, homeostatic scaling leads to elevated spontaneous firing rates. Constant additional (non-auditory) input to a cochlear nucleus neuron can boost the development of hyperactivity because this input is also amplified after hearing loss, as homeostasis is a global mechanism affecting all synapses that provide input to the neuron.

The model is in agreement with several animal studies demonstrating that acoustic trauma can lead to increased spontaneous firing rates in the DCN (Brozoski *et al*., 2002; Kaltenbach *et al*., 2004) and to behavioral signs of tinnitus (Brozoski *et al*., 2002; Heffner & Harrington, 2002; Kaltenbach *et al*., 2004). Interestingly, the strength of the behavioral evidence for tinnitus is correlated to the amount of hyperactivity in the DCN (Kaltenbach *et al*., 2004). The DCN, however, need not be the sole generator of tinnitus-related activity in the auditory system, as DCN ablation does not seem to abolish behavioral signs of tinnitus (Brozoski & Bauer, 2005). If the proposed mechanism of activity stabilization is relevant for various types of neurons along a sensory pathway, hyperactivity could arise at any stage that is confronted with decreased excitatory input. Ablation of the DCN, for example, removes excitatory input to subsequent stages such as the inferior colliculus. It is thus conceivable that homeostasis triggers hyperactivity there.

In our model, homeostatic plasticity restores the mean firing rate of a second-order auditory neuron after hearing loss. The fraction of time the neuron spends firing at its spontaneous rate, however, cannot be decreased by homeostasis or other plasticity mechanisms, because this fraction is fixed by the response threshold of AN fibers. This fact applies to all neurons along the auditory pathway. Therefore, even if homeostatic plasticity simultaneously occurs at several stages of the auditory system, pathological neuronal activity generated at one processing stage cannot be reverted to healthy activity distributions by homeostasis in subsequent stages. As spontaneous firing after hearing loss typically has a higher probability than before, its contribution to the mean activity is increased at all stages. Restoring the mean rate is therefore to be expected to increase the spontaneous rate throughout the auditory system.

Following sensory deprivation, indications of a homeostatic mechanism have indeed been seen at various stages of the auditory pathway. In the inferior colliculus of gerbils, for example, bilateral deafening leads to increased EPSC amplitudes and increased IPSC equilibrium potentials (Vale & Sanes, 2002), suggesting that the balance between excitation and inhibition is shifted in a homeostatic fashion. Moreover, in the cochlear nucleus of chinchillas, acoustic trauma temporarily increased glutamatergic synaptic transmission (Muly *et al*., 2004). Increased EPSC amplitudes were also observed in the anteroventral cochlear nucleus of congenitally deaf mice in response to electrical stimulation of the AN (Oleskevich & Walmsley, 2002). Furthermore, glycinergic inhibition in the DCN was persistently weakened following unilateral cochlear ablation (Suneja *et al*., 1998a, 1998b) or age-related hearing loss (Caspary *et al*., 2005). Finally, in the auditory cortex of gerbils, increased excitability as well as increased excitatory and decreased inhibitory synaptic transmission were measured after bilateral cochlear ablation (Kotak *et al*., 2005). Homeostatic plasticity may thus be involved in activity-dependent regulatory processes throughout the auditory system.

Further evidence for homeostasis-like mechanisms in the auditory pathway comes from the observed time scale of changes after sensory deprivation. Hyperactivity in the DCN develops within days after hearing loss. Although cochlear damage and thus the auditory threshold shift is already present two days after acoustic trauma, no increase in DCN spontaneous firing rates is observed at that time (Kaltenbach *et al*., 1998). Five days after acoustic trauma, however, hyperactivity is fully developed (Kaltenbach *et al*., 2000). This finding indicates that homeostatic plasticity could be involved, as changes through homeostasis also occur on a time-scale of days (Turrigiano *et al*., 1998). Reminiscent of homeostatic plasticity, Formby *et al*. (2003) found a gain control mechanism that regulates loudness perception depending on the overall amount of sensory input to the human auditory system. The gain control operated, again, on a time-scale of days.

Homeostatic regulation of neuronal activity levels might be a general principle in sensory pathways. In the visual system of rats (postnatal day 15), hyperactivity of cortical neurons has been observed after two days of visual deprivation (Maffei *et al*., 2004): excitatory synaptic connections were strengthened, inhibitory synapses were weakened, and the spontaneous firing rates of specific cortical neurons were increased; restoring vision reversed the changes. In the somatosensory system, our findings might also be applicable to the phenomenon of phantom limb sensations that can arise after amputations. Another modelling study indicates that homeostatic plasticity after deafferentiation could be involved in post-traumatic epileptogenesis (Houweling *et al*., 2005).

To demonstrate that homeostatic plasticity after hearing loss can lead to increased spontaneous firing rates in second-order neurons, we deliberately chose a phenomenological modelling approach that is based on several simplifying assumptions. In our model of the AN population rate, for example, the shape of the rate-intensity function is coupled to the shape of the intensity distribution by the infomax tuning assumption. This results in a steepening of rate-intensity functions for elevated thresholds, which matches observations for isolated OHC loss (Harrison, 1981). SD also elevates thresholds, but single AN fibers can display rate-intensity functions that are even shallower than normal (Heinz & Young, 2004). Shallower rate-intensity functions, however, would lead to a greater reduction of the mean AN rate. In our model, more homeostatic compensation would then be needed in second-order neurons, resulting in more hyperactivity. Thus, for the development of hyperactivity, steepening of the rate-intensity functions is the more conservative assumption. Another simplifying assumption in our model is that we consider only excitatory input, whereas neurons in the CN are part of an elaborate circuitry containing a variety of inhibitory interneurons (Rhode & Greenberg, 1992; Young & Davis, 2002). This is most evident, for example, in the responses of type IV neurons of the DCN, which are characterized by inhibitory sidebands and nonmonotonic rate-intensity functions (Spirou & Young, 1991; Young & Davis, 2002). Because neurons in the cochlear nucleus are part of a sensory pathway, it is likely that even for such

complex response properties the net effect of natural acoustic stimuli is excitatory, leading to a mean firing rate that is above the spontaneous one. It is unknown how the mean firing rate of these neurons changes as a result of hearing loss in behaving animals, and firing statistics of auditory neurons in natural environments are not available. However, we regard it as reasonable that cochlear damage decreases the mean activity level in a large fraction of neurons in the cochlear nucleus. Decreased mean activity could then trigger homeostatic plasticity, leading to increased spontaneous firing rates. This conclusion is independent of details of information processing in the auditory pathway.

The presented model is as simple as possible to exhibit the consequences of homeostatic plasticity in the auditory system. The model therefore has no free parameters, that is, parameters do not need to be fitted. Several extensions of the model are possible in order to test whether its features are robust with respect to more biophysical details. A more detailed model of the basilar membrane, hair cells and the auditory nerve could be used (Zhang *et al*., 2001; Sumner *et al*., 2003). The second-order neuron could be described through a conduction-based unit (Kanold & Manis, 2001), and inserted into a neuronal network with inhibition (Reed & Blum, 1995; Blum & Reed, 1998; Franosch *et al*., 2003). Finally, feedback through the efferent auditory system could be considered, and other damage and plasticity mechanism could be incorporated, like excitotoxicity and subsequent sprouting of new synapses, or long-term potentiation and depression at individual synapses. Also the time-course of homeostatic plasticity could be investigated. These extensions are, however, way beyond the scope of this article. Such extensions would lead to large amount of additional parameters that would add many degrees of freedom to the model, which need to be reasonably constrained to reach viable predictions. That is why we chose to utilize a minimal model that emphasizes the most important features of this complex system. Nevertheless, we hope that the presented model provides a basis for deriving more detailed models of tinnitus development.

Even though our model is extremely simple, the relation between the pattern of cochlear damage and the resulting profile of hyperactivity in a tonotopic array of model neurons matches observations in the DCN of animals (e.g. Kaltenbach *et al*., 2002). We note that for stereocilia damage resembling noise-induced hearing loss, the model generates activity peaks in neurons with best frequencies above the edge of the cochlear lesion. These peaks could be interpreted as a basis for tinnitus sensations with tonal characteristics and a pitch at a frequency where cochlear damage/hearing loss exceeds a certain degree. A similar association between tinnitus pitch (Henry *et al*., 1999) or tinnitus spectrum (Norena *et al*., 2002) and the extent of hearing loss has been observed in humans. It is still unclear, however, why some patients with hearing loss develop tinnitus whereas others do not. Moreover, not all tinnitus patients have impaired hearing, although there is evidence that tinnitus patients without obvious signs of hearing loss might have restricted cochlear damage that is not detected by conventional audiometry (Weisz *et al*., 2005). Our work indicates that the exact type and spatial pattern of cochlear damage as well as the strength of non-auditory inputs are crucial for the development of hyperactivity. In human subjects, however, information on the type and amount of cochlear damage can only be obtained indirectly and to a very limited extent, and little is known about the variability of non-auditory inputs to the auditory pathway.

The proposed model for the development of hyperactivity complements the so-called 'Neurophysiological Model', which assumes that a tinnitus percept is generated by abnormal neuronal activity in the auditory periphery that is amplified through attentional and emotional processes (Jastreboff, 1999). From the 'Neurophysiological Model', the Tinnitus Retraining Therapy has been derived (Jastreboff & Jastreboff, 1999), which uses a combination of psychological counseling with masking devices and hearing aids. Our model explains why hearing loss can induce increased spontaneous firing rates in the early auditory pathway that may constitute the basis of a tinnitus sensation, and it also provides a biologically plausible and consistent framework for understanding how tinnitus-related hyperactivity might be reduced through appropriate external stimulation. We hope that this understanding will lead to improved strategies for a treatment of tinnitus.

Acknowledgements

We would like to thank Manfred Gross, Andreas Herz, Ovidiu König, Paula Kuokkanen, Christian Leibold, and Martin Stemmler for most helpful discussions on this work. This research was supported by the Deutsche Forschungsgemeinschaft (Emmy Noether Programm: Ke 788/1–3, SFB 618 'Theoretical Biology', TP B3) and the Bundesministerium für Bildung und Forschung (Bernstein Center for Computational Neuroscience Berlin, 01GQ0410).

Abbreviations

AN, auditory nerve; CF, characteristic frequency; CN, cochlear nucleus; DCN, dorsal cochlear nucleus; IHC, inner hair cell; OHC, outer hair cell; SD, stereocilia damage.

References

Blum, J.J. & Reed, M.C. (1998) Effects of wide band inhibitors in the dorsal cochlear nucleus. II. Model calculations of the responses to complex sounds. *J. Acoust. Soc. Am.*, **103**, 2000–2009.

Brozoski, T.J. & Bauer, C.A. (2005) The effect of dorsal cochlear nucleus ablation on tinnitus in rats. *Hear. Res.*, **206**, 227–236.

Brozoski, T.J., Bauer, C.A. & Caspary, D.M. (2002) Elevated fusiform cell activity in the dorsal cochlear nucleus of chinchillas with psychophysical evidence of tinnitus. *J. Neurosci.*, **22**, 2383–2390.

Burrone, J. & Murthy, V.N. (2003) Synaptic gain control and homeostasis. *Curr. Opin. Neurobiol.*, **13**, 560–567.

Cant, N.B. & Gaston, K.C. (1982) Pathways connecting the right and left cochlear nuclei. *J. Comp. Neurol.*, **212**, 313–326.

Caspary, D.M., Schatteman, T.A. & Hughes, L.F. (2005) Age-related changes in the inhibitory response properties of dorsal cochlear nucleus output neurons: role of inhibitory inputs. *J. Neurosci.*, **25**, 10952–10959.

Chen, G.D. & Fechter, L.D. (2003) The relationship between noise-induced hearing loss and hair cell loss in rats. *Hear. Res.*, **177**, 81–90.

Dallos, P. & Harris, D. (1978) Properties of auditory nerve responses in absence of outer hair cells. *J. Neurophysiol.*, **41**, 365–383.

Desai, N.S., Rutherford, L.C. & Turrigiano, G.G. (1999) Plasticity in the intrinsic excitability of cortical pyramidal neurons. *Nature Neurosci.*, **2**, 515–520.

Escabi, M.A., Miller, L.M., Read, H.L. & Schreiner, C.E. (2003) Naturalistic auditory contrast improves spectrotemporal coding in the cat inferior colliculus. *J. Neurosci.*, **23**, 11489–11504.

Formby, C., Sherlock, L. & Gold, S.L. (2003) Adaptive plasticity of loudness induced by chronic attenuation and enhancement of the acoustic background. *J. Acoust. Soc. Am.*, **114**, 55–58.

Franosch, J.-M.P., Kempter, R., Fastl, H. & van Hemmen, J.L. (2003) Zwicker tone illusion and noise reduction in the auditory system. *Phys. Rev. Lett.*, **90**, 178103.

Geisler, C.D. (1998) *From Sound to Synapse*. Oxford University Press, New York.

Harrison, R.V. (1981) Rate-versus-intensity functions and related AP responses in normal and pathological guinea pig and human cochleas. *J. Acoust. Soc. Am.*, **70**, 1036–1044.

Hazell, J.W.P. (1999) The TRT method in practice. In Hazell, J.W.P., (Ed) *Proceedings of the Sixth International Tinnitus Seminar.* The Tinnitus and Hyperacusis Centre, London, pp. 92–98.

Heffner, H.E. & Harrington, I.A. (2002) Tinnitus in hamsters following exposure to intense sound. *Hear. Res.*, **170**, 83–95.
Heinz, M.G. & Young, E.D. (2004) Response growth with sound level in auditory nerve fibers after noise-induced hearing loss. *J. Neurophysiol.*, **91**, 784–794.
Henry, J.A., Meikle, M. & Gilbert, A. (1999) Audiometric correlates of tinnitus pitch: insights from the Tinnitus Data Registry. In Hazell, J.W.P., (Ed), *Proceedings of the Sixth International Tinnitus Seminar.* The Tinnitus and Hyperacusis Centre, London, pp. 51–57.
Houweling, A.R., Bazhenov, M., Timofeev, I., Steriade, M. & Sejnowski, T.J. (2005) Homeostatic synaptic plasticity can explain post-traumatic epileptogenesis in chronically isolated neocortex. *Cereb. Cortex*, **15**, 834–845.
Ito, J. & Sakakihara, J. (1994) Suppression of tinnitus by cochlear implantation. *Am. J. Otolaryngol.*, **15**, 145–148.
Jacomme, A.V., Nodal, F.R., Bajo, V.M., Manunta, Y., Edeline, J.M., Babalian, A. & Rouiller, E.M. (2003) The projection from auditory cortex to cochlear nucleus in guinea pigs: an *in vivo* anatomical and *in vitro* electrophysiological study. *Exp. Brain Res.*, **153**, 467–476.
Jastreboff, P.J. (1999) The neurophysiological model of tinnitus and hyperacusis. In Hazell, J.W.P., (Ed), *Proceedings of the Sixth International Tinnitus Seminar.* The Tinnitus and Hyperacusis Centre, London, pp. 32–38.
Jastreboff, M.M. & Jastreboff, P.J. (1999) How TRT derives from the neurophysiological model. In Hazell, J.W.P. (Ed), *Proceedings of the Sixth International Tinnitus Seminar.* The Tinnitus and Hyperacusis Centre, London, pp. 87–91.
Kaltenbach, J.A. & Afman, C.E. (2000) Hyperactivity in the dorsal cochlear nucleus after intense sound exposure and its resemblance to tone-evoked activity: a physiological model for tinnitus. *Hear. Res.*, **140**, 165–172.
Kaltenbach, J.A., Godfrey, D.A., Neumann, J.B., McCaslin, D.L., Afman, C.E. & Zhang, J. (1998) Changes in spontaneous neural activity in the dorsal cochlear nucleus following exposure to intense sound: relation to threshold shift. *Hear. Res.*, **124**, 78–84.
Kaltenbach, J.A., Rachel, J.D., Mathog, T.A., Zhang, J., Falzarano, P.R. & Lewandowski, M. (2002) Cisplatin-induced hyperactivity in the dorsal cochlear nucleus and its relation to outer hair cell loss: relevance to tinnitus. *J. Neurophysiol.*, **88**, 699–714.
Kaltenbach, J.A., Zacharek, M.A., Zhang, J. & Frederick, S. (2004) Activity in the dorsal cochlear nucleus of hamsters previously tested for tinnitus following intense tone exposure. *Neurosci. Lett.*, **355**, 121–125.
Kaltenbach, J.A., Zhang, J. & Afman, C.E. (2000) Plasticity of spontaneous neural activity in the dorsal cochlear nucleus after intense sound exposure. *Hear. Res.*, **147**, 282–292.
Kanold, P.O. & Manis, P.B. (2001) A physiologically based model of discharge pattern regulation by transient K^+ currents in cochlear nucleus pyramidal cells. *J. Neurophysiol.*, **85**, 523–538.
Kanold, P.O. & Young, E.D. (2001) Proprioceptive information from the pinna provides somatosensory input to cat dorsal cochlear nucleus. *J. Neurosci.*, **21**, 7848–7858.
Kilman, V., van Rossum, M.C.W. & Turrigiano, G.G. (2002) Activity deprivation reduces miniature IPSC amplitude by decreasing the number of postsynaptic $GABA_A$ receptors clustered at neocortical synapses. *J. Neurosci.*, **22**, 1328–1337.
Kotak, V.C., Fujisawa, S., Lee, F.A., Karthikeyan, O., Aoki, C. & Sanes, D.H. (2005) Hearing loss raises excitability in the auditory cortex. *J. Neurosci.*, **25**, 3908–3918.
Laughlin, S. (1981) A simple coding procedure enhances a neuron's information capacity. *Z. Naturforsch.*, **36**, 910–912.
Liberman, M.C. (1978) Auditory-nerve response from cats raised in a low-noise chamber. *J. Acoust. Soc. Am.*, **63**, 442–455.
Liberman, M.C. (1984) Single-neuron labeling and chronic cochlear pathology. I. Threshold shift and characteristic-frequency shift. *Hear. Res.*, **16**, 33–41.
Liberman, M.C. & Dodds, L.W. (1984) Single-neuron labeling and chronic cochlear pathology. II. Stereocilia damage and alterations of spontaneous discharge rates. *Hear. Res.*, **16**, 43–53.
Liberman, M.C. & Kiang, N.Y. (1984) Single-neuron labeling and chronic cochlear pathology. IV. Stereocilia damage and alterations in rate- and phase-level functions. *Hear. Res.*, **16**, 75–90.
Maffei, A., Nelson, S.B. & Turrigiano, G.G. (2004) Selective reconfiguration of layer 4 visual cortical circuitry by visual deprivation. *Nature Neurosci.*, **7**, 1353–1359.
Meleca, R.J., Kaltenbach, J.A. & Falzarano, P.R. (1997) Changes in the tonotopic map of the dorsal cochlear nucleus in hamsters with hair cell loss and radial nerve bundle degeneration. *Brain Res.*, **750**, 201–213.
Muly, S.M., Gross, J.S. & Potashner, S.J. (2004) Noise trauma alters D-[3H]aspartate release and AMPA binding in chinchilla cochlear nucleus. *J. Neurosci. Res.*, **75**, 585–596.
Noreña, A.J. & Eggermont, J.J. (2003) Changes in spontaneous neural activity immediately after an acoustic trauma: implications for neural correlates of tinnitus. *Hear. Res.*, **183**, 137–153.
Norena, A., Micheyl, C., Chery-Croze, S. & Collet, L. (2002) Psychoacoustic characterization of the tinnitus spectrum: implications for the underlying mechanisms of tinnitus. *Audiol. Neurootol.*, **7**, 358–369.
Oleskevich, S. & Walmsley, B. (2002) Synaptic transmission in the auditory brainstem of normal and congenitally deaf mice. *J. Physiol.*, **540**, 447–455.
Pilgramm, M., Rychlik, R., Siedentrop, H., Goebel, G. & Kirchhoff, D. (1999) Tinnitus in the Federal Republic of Germany: a representative epidemological study. In Hazell, J.W.P., (Ed), *Proceedings of the Sixth International Tinnitus Seminar.* The Tinnitus and Hyperacusis Centre, London, pp. 64–67.
Quaranta, N., Wagstaff, S. & Baguley, D.M. (2004) Tinnitus and cochlear implantation. *Int. J. Audiol.*, **43**, 245–251.
Reed, M.C. & Blum, J.J. (1995) A computational model for signal processing by the dorsal cochlear nucleus. I. Responses to pure tones. *J. Acoust. Soc. Am.*, **97**, 425–438.
Rhode, W.S. & Greenberg, S. (1992) Physiology of the cochlear nuclei. In Oertel, D., Fay, R.R. & Popper, A.N., (Eds), *The Mammalian Auditory Pathway: Neurophysiology 2 of Springer Handbook of Auditory Research.* Springer, New York, pp. 94–152.
van Ruijven, M.W., de Groot, J.C., Klis, S.F. & Smoorenburg, G.F. (2005) The cochlear targets of cisplatin: an electrophysiological and morphological time-sequence study. *Hear. Res.*, **205**, 241–248.
van Ruijven, M.W., de Groot, J.C. & Smoorenburg, G. (2004) Time sequence of degeneration pattern in the guinea pig cochlea during cisplatin administration. A quantitative histological study. *Hear. Res.*, **197**, 44–54.
Ryugo, D.K. (1992) The auditory nerve: peripheral innervation, cell body morphology, and central projections. In Webster, D., Popper, A. & Fay, R., (Eds), *The Mammalian Auditory Pathway, Neuroanatomy.* Springer, New York, pp. 23–65.
Sachs, M.B. & Abbas, P.J. (1974) Rate versus level functions for auditory-nerve fibers in cats: tone-burst stimuli. *J. Acoust. Soc. Am.*, **56**, 1835–1847.
Salvi, R.J., Wang, J. & Ding, D. (2000) Auditory plasticity and hyperactivity following cochlear damage. *Hear. Res.*, **147**, 261–274.
Schmiedt, R.A. & Zwislocki, J.J. (1980) Effects of hair cell lesions on responses of cochlear nerve fibers. II. Single- and two-tone intensity functions in relation to tuning curves. *J. Neurophysiol.*, **43**, 1390–1405.
Schneider, E., Hocker, K.M., Lebisch, H. & Pilgramm, M. (1999) Does systematic noise stimulation improve tinnitus habituation? In Hazell, J.W.P. (Ed), *Proceedings of the Sixth International Tinnitus Seminar.* The Tinnitus and Hyperacusis Centre, London, pp. 391–393.
Seki, S. & Eggermont, J.J. (2002) Changes in cat primary auditory cortex after minor-to-moderate pure-tone induced hearing loss. *Hear. Res.*, **173**, 172–186.
Seki, S. & Eggermont, J.J. (2003) Changes in spontaneous firing rate and neural synchrony in cat primary auditory cortex after localized tone-induced hearing loss. *Hear. Res.*, **180**, 28–38.
Shore, S.E., Godfrey, D.A., Helfert, R.H., Altschuler, R.A. & Bledsoe, S.C.J. (1992) Connections between the cochlear nuclei in guinea pig. *Hear. Res.*, **62**, 16–26.
Spirou, G.A. & Young, E.D. (1991) Organization of dorsal cochlear nucleus type IV unit response maps and their relationship to activation by bandlimited noise. *J. Neurophysiol.*, **66**, 1750–1768.
Sumner, C.J., O'Mard, L.P., Lopez-Poveda, E.A. & Meddis, R. (2003) A nonlinear filter-bank model of the guinea-pig cochlear nerve: rate responses. *J. Acoust. Soc. Am.*, **113**, 3264–3274.
Suneja, S.K., Benson, C.G. & Potashner, S.J. (1998a) Glycine receptors in adult guinea pig brain stem auditory nuclei: regulation after unilateral cochlear ablation. *Exp. Neurol.*, **154**, 473–488.
Suneja, S.K., Potashner, S.J. & Benson, C.G. (1998b) Plastic changes in glycine and GABA release and uptake in adult brain stem auditory nuclei after unilateral middle ear ossicle removal and cochlear ablation. *Exp. Neurol.*, **151**, 273–288.
Surr, R.K., Kolb, J.A., Cord, M.T. & Garrus, N.P. (1999) Tinnitus handicap inventory (THI) as a hearing aid outcome measure. *J. Am. Acad. Audiol.*, **10**, 489–495.
Turrigiano, G.G. (1999) Homeostatic plasticity in neuronal networks: the more things change, the more they stay the same. *Trends Neurosci.*, **22**, 221–227.
Turrigiano, G.G., Leslie, K.R., Desai, N.S., Rutherford, L.C. & Nelson, S.B. (1998) Activity-dependent scaling of quantal amplitude in neocortical neurons. *Nature*, **391**, 892–896.

Vale, C. & Sanes, D.H. (2002) The effect of bilateral deafness on excitatory and inhibitory synaptic strength in the inferior colliculus. *Eur. J. Neurosci.*, **16**, 2394–2404.

Wang, J., Ding, D. & Salvi, R.J. (2002a) Functional reorganization in chinchilla inferior colliculus associated with chronic and acute cochlear damage. *Hear. Res.*, **168**, 238–249.

Wang, Y., Hirose, K. & Liberman, M.C. (2002b) Dynamics of noise-induced cellular injury and repair in the mouse cochlea. *J. Assoc. Res. Otolaryngol.*, **3**, 248–268.

Wang, J., Powers, N.L., Hofstetter, P., Trautwein, P., Ding, R. & Salvi, R. (1997) Effects of selective inner hair cell loss on auditory nerve fiber threshold, tuning and spontaneous and driven discharge rate. *Hear. Res.*, **107**, 67–82.

Weedman, D.L. & Ryugo, D. (1996) Pyramidal cells in primary auditory cortex project to cochlear nucleus in rat. *Brain Res.*, **706**, 97–102.

Weisz, N., Hartmann, T., Dohrmann, K., Schlee, N. & Norena, A. (2005) Psychoacoustic evidence for deafferentiation in tinnitus subjects with normal audiograms. In Dauman, R. & Bouscau-Faure, F., (Eds), *Proceedings of the VIIIth International Tinnitus Seminar*, *Pau France, September 2005.* The French Society for Audiology, Paris, France, p.76.

Young, E.D. & Davis, K.A. (2002) Circuitry and function of the dorsal cochlear nucleus. In Oertel, D., Fay, R.R. & Popper, A.N., (Eds), *Integrative Functions in the Mammalian Auditory Pathway 15 of Springer Handbook of Auditory Research.* Springer, New York, pp. 121–157.

Zacharek, M.A., Kaltenbach, J.A., Mathog, T.A. & Zhang, J. (2002) Effects of cochlear ablation on noise induced hyperactivity in the hamster dorsal cochlear nucleus: implications for the origin of noise induced tinnitus. *Hear. Res.*, **172**, 137–144.

Zhang, X., Heinz, M.G., Bruce, I.C. & Carney, L.H. (2001) A phenomenological model for the responses of auditory nerve fibers: I. Non-linear tuning with compression and suppression. *J. Acoust. Soc. Am.*, **109**, 648–670.

Zhou, J. & Shore, S. (2004) Projections from the trigeminal nuclear complex to the cochlear nuclei: a retrograde and anterograde tracing study in the guinea pig. *J. Neurosci. Res.*, **78**, 901–907.